Journal of Materials Chemistry A

PAPER

View Article Online
View Journal | View Issue

Cite this: J. Mater. Chem. A, 2017, 5, 1168

A multi-aromatic hydrocarbon unit induced hydrophobic metal–organic framework for efficient C_2/C_1 hydrocarbon and oil/water separation†

Minghui Zhang,[ab] Xuelian Xin,[b] Zhenyu Xiao,[b] Rongming Wang,*[ab] Liangliang Zhang[a] and Daofeng Sun*[ab]

Received 27th September 2016
Accepted 3rd December 2016

DOI: 10.1039/c6ta08368d

www.rsc.org/MaterialsA

Oil spills have led to more and more energy waste and economic losses all over the world. Developing highly hydrophobic materials for efficient oil/water separation has become key in solving this global issue. Here we report a highly hydrophobic porous metal–organic framework, named **UPC-21**, constructed from a pentiptycene-based organic ligand, for efficient oil/water separation. Large and pure crystals of **UPC-21** could be obtained with high yield through a developed "diauxic growth" strategy. Due to the existence of multi-aromatic hydrocarbon units in the central pentiptycene core of the ligand, **UPC-21** exhibits high hydrophobicity with a water contact angle of 145 ± 1° and superoleophilicity with an oil contact angle of 0°. Strikingly, oil/water separation measurements reveal that **UPC-21** can efficiently separate toluene/water, hexane/water, gasoline/water, naphtha/water, and crude oil/water with a separation efficiency being above 99.0% except for crude oil/water due to its high viscosity and complex composition. Our work presented here may open a new avenue for the application of porous MOF materials.

Introduction

The energy crisis, along with environmental pollution, seriously threatens the development of human society. Energy conservation and environmental protection have thus become issues of global concern.[1–3] As is well-known, oil and petroleum hydrocarbon products are currently the most important energy sources and raw materials in the world. However, oil spill accidents have not only led to the loss of energy but also caused serious environmental pollution.[4–8] For example, the largest oil spill occurred in 2010, releasing about 4.9 million barrels of Southern Louisiana crude oil into the Gulf of Mexico, resulting in vast economic losses and significant environmental damage. Actually, the global clean-up costs arising from oil spill accidents exceeded 10 billion dollars annually.[9–11] Therefore, it has become imperative to develop effective methods[12,13] for cleaning up oil to reduce the long-term effects of environmental pollution by these oil spills. Compared to the burning of oil, effective oil/water separation seems to be a favoured option, since the spilled oil can be recovered and reused in industries without causing any environmental pollution *via* this physical method.[14–17] Among the various systems developed for the oil/water separation process, such as filtration, gravity separation, electrochemical methods and flotation, it has been found that filtration may hold a greater advantage, owing to its simplicity, low cost and high efficiency.[18–22] Although many adsorbents such as sand and organoclays have also been used in oil spill clean-ups in the past decade, the strong affinity of these materials to water limits their effectiveness in the treatment of oil spills. Thus, developing new hydrophobic adsorbents to be used for oil spill clean-ups remains an urgent challenge. On the other hand, the separation of C_2 and C_3 hydrocarbons from CH_4 is an important industrial process,[23–27] due to the high quality and purity requirements for their practical usage.[28–32] However, the traditional separation technology is based on the difference of vapor pressures of light hydrocarbons, which is very energy-intensive. Compared to the traditional separation technologies, adsorptive separation is one of the most promising energy-efficient routes. Hence, developing new-type adsorbents for the separation of light hydrocarbons is also an important subject.[33–37]

Porous metal–organic frameworks (MOFs), or coordination polymers, are a new type of promising adsorbents for many guest molecules such as CO_2, H_2, CH_4, and O_2 and have been widely used in gas storage and separation.[38–42] The biggest advantage of MOFs over other porous materials such as activated carbon and zeolites is the high surface area and the

[a]State Key Laboratory of Heavy Oil Processing, College of Science, China University of Petroleum (East China), Qingdao, Shandong 266580, People's Republic of China. E-mail: rmwang@upc.edu.cn; dfsun@upc.edu.cn

[b]College of Science, China University of Petroleum (East China), Qingdao, Shandong 266580, People's Republic of China

† Electronic supplementary information (ESI) available. See DOI: 10.1039/c6ta08368d

tunable chemical and physical properties of the pores.[43–45] Actually, a large number of functional MOFs with high H_2/CH_4 storage or CO_2 capture and separation efficiency were synthesized and reported by introducing functional groups to coat the surface of the pores.[46–49] However, the requirement of MOF materials for the application in oil/water separation is quite different to that in gas storage/separation. The wettability of the MOF surface is very crucial to oil/water separation. The MOF surfaces with (super)hydrophobicity or (super)oleophilicity are beneficial to the removal of oil from water.[50] Unfortunately, most porous MOFs are moisture-sensitive and cannot retain their framework in water. Therefore, design and synthesis of both hydrophobic and water-resistant MOF materials is an urgent need for the application in oil/water separation. On the basis of current research, there are two main strategies for the production of hydrophobic MOF materials: one is the utilization of hydrophobic linkers such as alkyl and/or fluorine-coated organic ligands to create porous MOFs; the other is the composite of porous MOFs combined with other hydrophobic materials such as highly fluorinated graphene oxide. In the past decade, a few very hydrophobic MOFs based on long-chain alkyl substituents and/or fluorine-coated ligands were reported.[51–53] In particular, superhigh hydrophobic fluorous MOFs with a high affinity to C_6–C_8 hydrocarbons of oil components were synthesized by the Omary Group. The Cohen Group reported a series of moisture-resistant and superhydrophobic MOFs through post-synthetic modification of long alkyl substituents on the organic ligands.[54] Recently, Kitagawa and coworkers designed a superhydrophobic porous coordination polymer by using an aromatic hydrocarbon building unit,[55] and the formation of corrugation by aromatic hydrocarbon on the external surface was thought to be responsible for the generation of superhydrophobic materials.

Although a few hydrophobic MOFs have been designed and synthesized recently, the direct application of hydrophobic MOFs on practical oil/water separation remains unexplored. Very recently, we designed a porous luminescent Cu(II) MOF (**UPC-21**), which represents the first pentiptycene-based 3D framework. Considering the existence of multi-aromatic hydrocarbon building units and open metal sites in **UPC-21** (Scheme 1), extended research on its hydrophobicity and separation properties was carried out. The results show that **UPC-21** is highly hydrophobic and exhibits excellent oil/water and light hydrocarbon separation efficiencies.

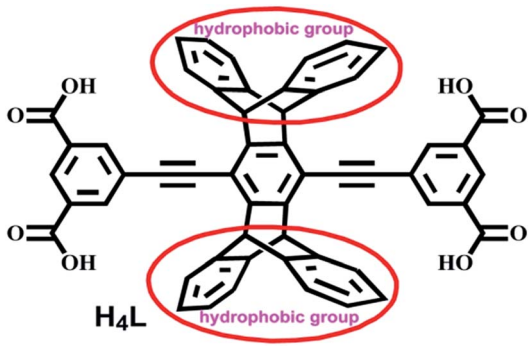

Scheme 1 H_4L ligand with dangling hydrophobic groups.

Results and discussion

Modified synthesis of UPC-21

UPC-21 was synthesized through a solvothermal reaction of H_4**L** and $Cu(NO_3)_2$ in the mixed DEF and H_2O in our previous report.[56] The crystals formed through this method are small, and the yield and purity seem somewhat unsatisfied (Fig. 1a). In our current research, the synthetic method was further modified through a "diauxic growth" strategy. H_4**L** and $Cu(NO_3)_2$ were dissolved in the mixed solvent of DEF and H_2O and sealed in a vial, which was placed in an oven at 75 °C for 25 hours. After cooling down to room temperature, the obtained small crystals were filtered and the filtrate (mother liquor) was poured back to the vial, which was further placed in an oven at 75 °C for another 25 hours. Large pure crystals of **UPC-21** were formed with a high yield (Fig. 1b). The purity and quality of the sample was further checked by P-XRD analysis (Fig. S1†) and nitrogen adsorption measurement. As shown in Fig. 1c and d, both samples display typical type-I adsorption isotherms, suggesting the retention of the microporous structures after the removal of solvates. The sample prepared as per the previous method can adsorb 288.6 $cm^3\ g^{-1}$ of N_2 at 77 K and 1 bar with the Brunauer–Emmett–Teller (BET) surface area of 1253.6 $m^2\ g^{-1}$. In contrast, the sample prepared through "diauxic growth" strategy can adsorb 448.0 $cm^3\ g^{-1}$ of N_2 at 77 K and 1 bar with the Brunauer–Emmett–Teller (BET) surface area of 1725.1 $m^2\ g^{-1}$, indicating that the quality of the sample is improved significantly after the modified synthesis.

Light hydrocarbon separation

The establishment of permanent porosity of **UPC-21** enables us to further examine its potential applications for the adsorption and separation of light hydrocarbons (C_1–C_3). Given the fact that copper open metal sites can enhance their interactions with

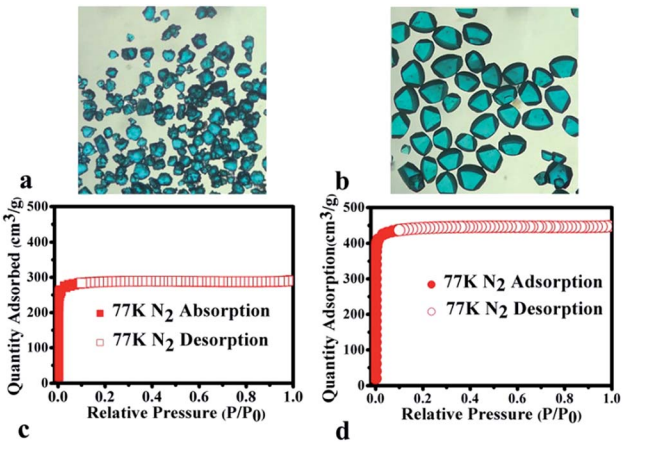

Fig. 1 The comparison of **UPC-21** before and after modified synthesis. Photograph of the single crystals of **UPC-21** before (a) and after (b) modified synthesis. The N_2 sorption isotherms for **UPC-21** at 77 K before (c) and after (d) modified synthesis.

acetylene,[57] thus we predicted that **UPC-21** would display higher storage capacities of acetylene. As shown in Fig. 2, **UPC-21** can take up acetylene up to 196.5 $cm^3\ g^{-1}$ at 273 K and 139.5 $cm^3\ g^{-1}$ at 295 K. Meanwhile, the uptake capacities of **UPC-21** for C_2H_4, C_2H_6, C_3H_6 and C_3H_8 are also fairly high at 273 K and 1 bar, with the values of 123.1, 137.6, 124.1, and 116.2 $cm^3\ g^{-1}$, respectively, whereas the corresponding values at 1 bar and 295 K are 98.4, 104.3, 110.1, and 103.0 $cm^3\ g^{-1}$, respectively. The uptake capacity of **UPC-21** for light hydrocarbons (C_2–C_3) at 295 K is much higher than those of the reported promising MOFs, such as M'MOF-3a,[53] UTSA-67a[58] and Cu(etz),[59] which is attributed to the synergistic effects of high density of open Cu(II) sites, multi-aromatic rings and the optimized pore size in **UPC-21**. The isosteric heats (Q_{st}) of adsorption at zero coverage, calculated based on the virial parameters, are 38.8, 24.7, and 23.1 kJ mol^{-1} for C_2H_2, C_2H_4, and C_2H_6, respectively (Fig. 2d), indicating the stronger interactions between the hydrocarbons and the coordination framework. On the other hand, **UPC-21** can adsorb only 43.2 and 25.7 $cm^3\ g^{-1}$ of CH_4 at 273 K and 295 K, respectively. The results indicate that **UPC-21** can selectively separate C_2 and C_3 hydrocarbons from CH_4. As shown in Fig. 3, the ideal adsorbed solution theory (IAST) was applied to estimate the C_2H_2/CH_4, C_2H_4/CH_4, C_2H_6/CH_4, C_3H_6/CH_4 and C_3H_8/CH_4 separation selectivities by fitting the experimental single component isotherms using a single site Langmuir–Freundlich model. When mixing C_2 (C_3) hydrocarbons and CH_4 equivalently, the calculated C_2H_2/CH_4, C_2H_4/CH_4, C_2H_6/CH_4, C_3H_6/CH_4 and C_3H_8/CH_4 molar ratio separation selectivities are 38.1, 23.5, 15.3, 75 and 67 at 298 K, respectively. It is worth noting that **UPC-21** exhibits much higher selectivity for C_2H_2/CH_4 than those previously reported MOFs at 295 K, such as MFM-130a[60] (34.7), UTSA-36a[61] (13.8), $Zn_4(OH)_2(1,2,4\text{-BTC})_2$ (ref. 62) (14.7) and $Zn_5(BTA)_6(TDA)_2$ (ref. 63) (15.5). Meanwhile, the C_2H_6/CH_4 selectivity for **UPC-21** (15.7) is also much higher than those reported MOFs with open metal sites, such as Cu(BTC) (HKUST-1) (11) and Mg-MOF-74 (14).[64]

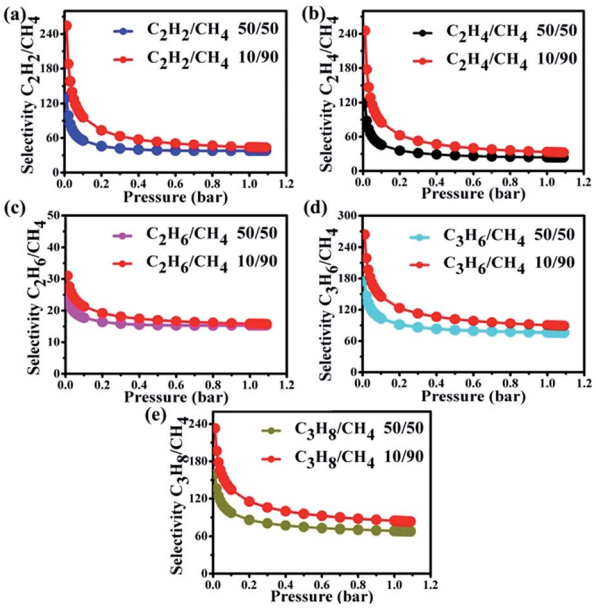

Fig. 3 Selective adsorption of **UPC-21**. The calculations of IAST selectivities for mixtures of C_2H_2/CH_4 (a), C_2H_4/CH_4 (b), C_2H_6/CH_4 (c), C_3H_6/CH_4 (d) and C_3H_8/CH_4 (e) at 295 K.

Structure and hydrophobicity of UPC-21

In addition, **UPC-21** is a three-dimensional porous framework based on multi-aromatic hydrocarbon units, which are prepared according to our previous work.[56] In the structure, six L^{4-} ligands connect twelve $Cu_2(COO)_4$ paddlewheel SBUs to generate a spindle-shaped cage (Fig. 4a), in which six paddlewheel SBUs sit on the equator and two other paddlewheel SBUs occupy two vertexes. A large number of benzene rings in the pentiptycene core of L^{4-} ligand are located inside the cage, resulting in a hydrophobic cavity. The spindle-shaped cages are further linked to each other to give rise to a 3D porous framework (Fig. 4b). It should be pointed out that the hydrophobic

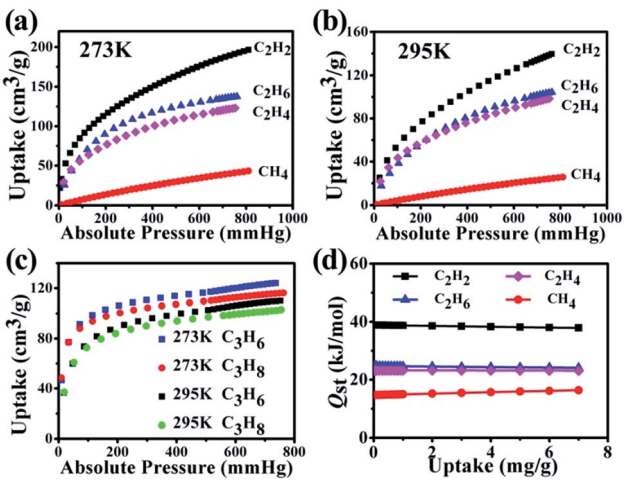

Fig. 2 Hydrocarbon adsorption of **UPC-21**. The C_2H_2, C_2H_4, C_2H_6 and CH_4 adsorption isotherms for **UPC-21** at 273 K (a) and 295 K (b). (c) The C_3H_6 and C_3H_8 adsorption isotherms for **UPC-21** at 273 K and 295 K. (d) The isosteric heat of adsorption for C_2H_2, C_2H_4, C_2H_6 and CH_4.

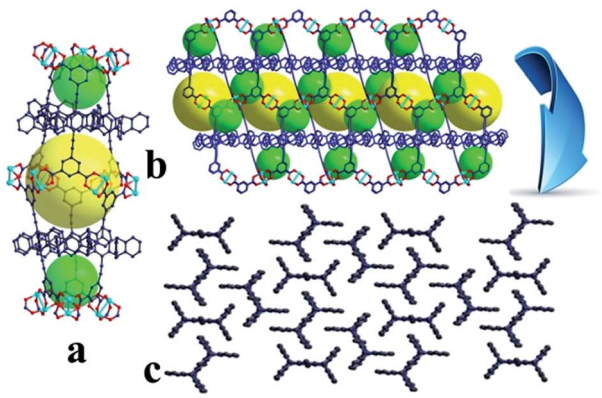

Fig. 4 X-ray crystal structure of **UPC-21**. (a) The spindle-shaped cage made up of six L^{4-} ligands connects twelve $Cu_2(COO)_4$ paddlewheel SBUs. (b) The 3D porous framework of **UPC-21** showing the arrangement of the spindle-shaped cages. (c) The highlights of the arrangement of the 2D layer pentiptycene cores of L^{4-} ligands in the 3D framework.

pentiptycene cores of L^{4-} ligands are arranged in a 2D layer (Fig. 4c), which is responsible for the generation of hydrophobic character of **UPC-21**.

Given the existence of multi-aromatic hydrocarbon units in **UPC-21**, the hydrophobicity investigation was also carried out by various experiments. As is well-known, most of the porous MOFs such as the two representatives, HKUST-1 with $Cu_2(COO)_4$ paddlewheel SBU and MOF-5 with $Zn_4O(COO)_6$ cluster, are hydrophilic and usually water/moisture sensitive.[21] Therefore, the water contact angles for these MOFs materials are normally close to 0°. Significantly, **UPC-21** exhibits a water contact angle of 145 ± 1°, suggesting its highly hydrophobic character. On the basis of current research on hydrophobic materials, most of the MOF bearing grafted aromatic ligands decorated with long alkyl chains such as MIL-53(Al)-AM series and SIM-2-(C_{12}) possess a contact angle of over 150° due to the presence of surface roughness and low-energy surfaces.[51] Compared to other hydrophobic MOFs (Table 1), the hydrophobicity of **UPC-21** is derived from the existence of multi-aromatic hydrocarbon units in the framework, which result in a bigger contact angle (145 ± 1°) than those of polyMOFs (110–120°)[24] and MOFs coated by polydimethysiloxane (130 ± 2°).[65]

To further confirm the hydrophobicity of **UPC-21**, dropwise addition of water or crude oil diluted by hexane onto the surface of **UPC-21** was carried out. As shown in Fig. 5a, when water was dropwise added onto the surface of **UPC-21** by using a syringe, the droplet of water was formed with a big contact angle, indicating its highly hydrophobic character. Furthermore, due to the surface tension, the crystals can be stuck to the surface of the droplet and form a water-in-crystal ball, which can roll off on a glass slide (Movie S1 in the ESI†). In contrast, the crude oil diluted by hexane can be rapidly adsorbed by **UPC-21**, suggesting its oleophilicity. Significantly, **UPC-21** can float on water for a long time without collapse (confirmed by powder XRD), but sink in ethyl acetate immediately, although the density of **UPC-21** is lower than that of ethyl acetate (Fig. 5b). Based on the above results, **UPC-21** is highly hydrophobic and oleophilic, and exhibits potential in oil/water separation.

Removal of pollutants from water

The permanent porosity, water stability and high hydrophobicity of **UPC-21** allow potential removal of a variety of organic pollutants from water. As shown in Fig. 6, a series of ultraviolet absorption experiments were carried out. Due to the especially low solubility of benzene and toluene in water, a set of approximately saturated solutions were obtained by adding excess benzene or toluene to 100 mL water. After dispersing **UPC-21** in the mixture for 6 h, 12 h, and 24 h, the UV/Vis spectra revealed that about 89.38% of benzene and 88.57% of toluene were adsorbed into the pores of **UPC-21**. These results suggest that **UPC-21** can efficiently remove organic pollutants from the water phase and thus exhibits the potential application in water purification.

Oil/water separation

Although a large number of hydrophobic MOFs were designed and synthesized in the past decade, study of hydrophobic MOFs on oil/water separation remains unexplored. Given that **UPC-21** is highly hydrophobic and oleophilic, a series of practical oil/water separation measurements were also carried out, as shown in Fig. 7 and Movie S2† for separation of gasoline/water without **UPC-21**, Movies S3–S7† for separation of toluene/water, hexane/water, gasoline/water, naphtha/water, and crude oil/water with **UPC-21** in the ESI.† Typically, a piece of gauze was put on the bottom of a syringe, on which was placed a crystal sample of **UPC-21**, and then another piece of gauze was put on the crystal sample to generate a simple filter. Since the organic objects including toluene, hexane, gasoline, naphtha and crude oil are lighter than water, they will remain on water and there is thus no contact with the crystals. To this end, the device was placed slantways to ensure the contact of the tested objects with the crystals. The toluene/water and hexane/water separations were first tested. When a mixture of water (dyed by acid red 18) and toluene or hexane was poured into the simple filter, toluene or hexane quickly passed through the crystal sample and fell into the vial beneath it, but water could not penetrate the hydrophobic crystals of **UPC-21**. Meanwhile, more and more toluene or hexane was collected in the vial to achieve the separation of toluene/water or hexane/water. Through the same procedure, separations of gasoline/water, naphtha/water and crude oil/water were also achieved successfully. After the separation, almost no visible signals of organic objects were observed in the water phase, indicating that the separation is highly efficient. To further confirm the performance of **UPC-21** on the oil/water separation, the separation efficiency was calculated using the oil rejection coefficient (R (%)) according to

$$R\ (\%) = \left(1 - \frac{C_p}{C_0}\right) \times 100$$

where C_0 and C_p are the oil concentration of the original oil/water mixtures and the collected water after the first separation, respectively. Based on the equation, the separation efficiency of **UPC-21** for a series of tested objects is above 99.0% except for crude oil, as shown in Table 2. The lower separation efficiency of crude oil may derive from the fact that the composition of crude oil is complex and the viscosity is higher than other tested objects. All the above results suggest that **UPC-21** exhibits oil/water separation with high efficiency. To the best of our knowledge, this is the first multi-aromatic hydrocarbon induced hydrophobic metal–organic framework exhibiting efficient oil/water separation.

Future focus and applications

Oil spills in oceans have led to a long-term threat to environment and human beings. Highly efficient oil/water separation is crucial to environmental protection and energy conservation. Although a large number of hydrophobic MOFs have been designed and synthesized in the past decade, study of this type of porous materials on oil/water separation is seldom. Given that porous MOFs exhibit large surface area, tunable pore functionality, easy synthesis and post modification, hydrophobic MOFs should have more advantage than other hydrophobic materials. **UPC-21** in this work is highly hydrophobic

Table 1 Water contact angle for **UPC-21** and other PCPs/MOFs

PCPs/MOFs	Surface modification Type	Structure of organic linker	Contact angle [°]	Ref.
PESD-1	Aromatic ring	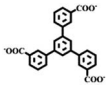	>150	55
MOFF-1	Fluorinated aromatic ring	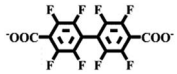	108 ± 2	54
MOFF-2	Fluorinated aromatic ring	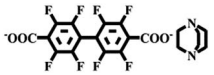	151 ± 1	54
MOFF-3	Fluorinated aromatic ring	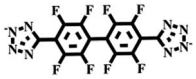	135 ± 2	54
IRMOF-3-AM4	Alkyl chain (C_4)	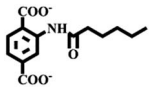	116 ± 6	51
IRMOF-3-AM5	Alkyl chain (C_5)	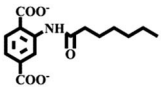	119 ± 10	51
IRMOF-3-AM6	Alkyl chain (C_6)	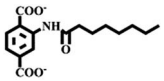	124 ± 8	51
IRMOF-3-AM15	Alkyl chain (C_{15})	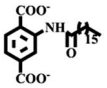	123 ± 5	51
IRMOF-3-AMiPr	Alkyl chain	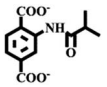	125 ± 12	51
IRMOF-3-AMiBu	Alkyl chain	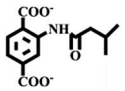	105 ± 11	51
MIL-53(Al)-AM4	Alkyl chain (C_4)	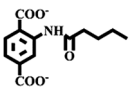	>150	51
MIL-53(Al)-AM6	Alkyl chain (C_6)	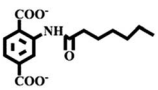	>150	51
HFGO@ZIF-8	Highly fluorinated graphene oxide		162	52
PDMS-MOF-5	Polydimethysiloxane coating	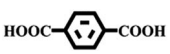	128	65
PDMS-HKUST-1	Polydimethysiloxane coating	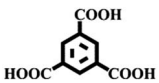	130	65
PDMS-ZnBT	Polydimethysiloxane coating	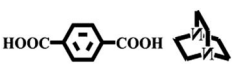	130	65
pbdc-9a	Alkyl chain (C_9)	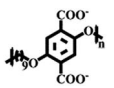	113 ± 2	66
pbdc-10a	Alkyl chain (C_{10})	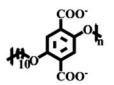	110 ± 1	66

Table 1 (*Contd.*)

PCPs/MOFs	Surface modification Type	Structure of organic linker	Contact angle [°]	Ref.
pbdc-11a	Alkyl chain (C_{11})	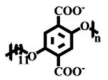	114 ± 1	66
pbdc-12a	Alkyl chain (C_{12})	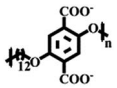	120 ± 2	66
UPC-21	Multi-aromatic rings	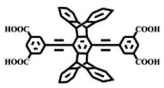	145 ± 1	This work

and exhibits high oil/water separation efficiency, which makes it a very promising material for oil/water separation and further opens a new avenue for the application of porous MOF materials. Introduction of more hydrophobic or special groups in the organic linkers to construct superhydrophobic MOFs materials is crucial to highly efficient oil/water separation or selective oil absorption, which is currently underway in our lab.

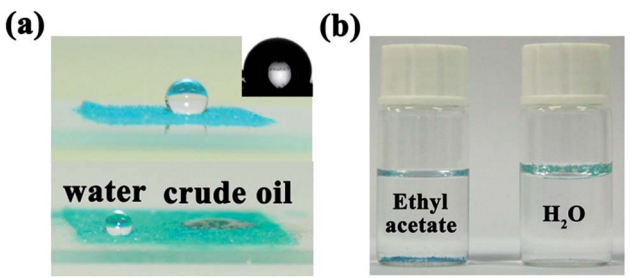

Fig. 5 Optical images of **UPC-21** showing the hydrophobic character. (a) The image of water droplet on the crystals of **UPC-21** (top), the inset image in the right-hand corner is the image of the static water droplet (5 μL) and the image of crude oil diluted by hexane dropped on the crystals of **UPC-21** (right). (b) Image of **UPC-21** that can float on the water (right) and sink in ethyl acetate (left).

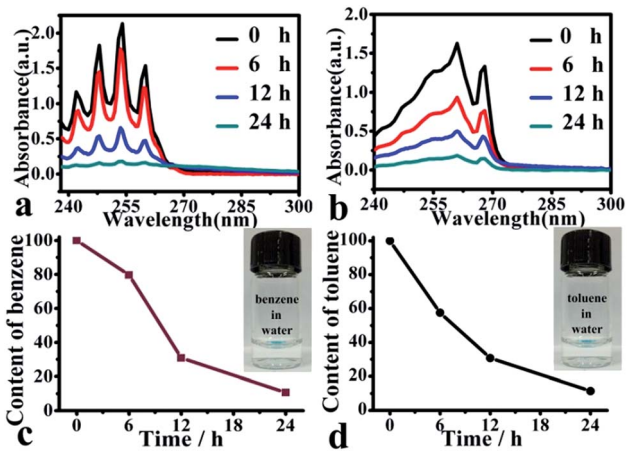

Fig. 6 UV-vis spectra of organic molecules in water. The change of UV-vis spectra for benzene (a) in water and toluene (b) in water with **UPC-21**. The absorbance curves of **UPC-21** for benzene (c) and toluene (d) from water.

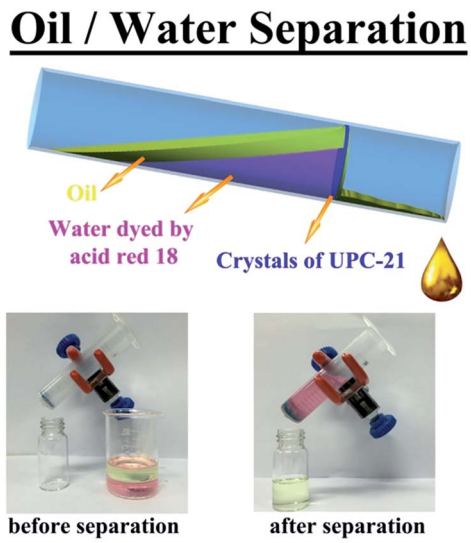

Fig. 7 Photographs showing the status of separation experiments. Oil/water separation efficiency. Water was colored with acid red 18 for clear observation.

Table 2 The separation efficiency for organic solvents and oils by **UPC-21**

	C_0	C_p	R (%)
Toluene	0.510	0.003	99.4
Hexane	0.505	0.004	99.2
Gasoline	0.524	0.005	99.0
Naphtha	0.498	0.004	99.2
Crude oil	0.514	0.012	97.6

Conclusions

The foregoing results have implications for the design and synthesis of future MOF materials for oil/water separation and selective oil absorption. The introduction of multi-aromatic hydrocarbon units in the organic ligand is responsible for the

formation of hydrophobic material **UPC-21**. Although porous MOF materials with high gas storage/separation, catalysis and luminescent sensors have been widely studied in the past few decades, **UPC-21** represents the first porous hydrophobic MOF that can be potentially applied in efficient oil/water separation.

Acknowledgements

This work was supported by the NSFC (Grant No. 21371179 and 21571187), NCET-11-0309, the Shandong Natural Science Fund for Distinguished Young Scholars (JQ201003), and the Fundamental Research Funds for the Central Universities (13CX05010A and 14CX02150A).

Notes and references

1 A. Mvungi, R. K. Hranova and D. Love, *Phys. Chem. Earth*, 2003, **28**, 1131–1137.
2 G. Y. Qing and T. L. Sun, *Adv. Mater.*, 2011, **23**, 1615–1620.
3 B. Wang, W. X. Liang, G. Z. Guo and W. M. Liu, *Chem. Soc. Rev.*, 2015, **44**, 336–361.
4 X. A. Alvarez-Salgado, J. L. Herrera, J. Gago, P. Otero, J. A. Soriano, C. G. Pola and C. Garcia-Soto, *Mar. Pollut. Bull.*, 2006, **53**, 239–249.
5 J. W. Short, S. D. Rice, R. A. Heintz, M. G. Carls and A. Mole, *Energy Sci.*, 2003, **25**, 509–517.
6 B. Dubansky, A. Whitehead, J. Miller, C. D. Rice and F. Galvez, *Environ. Sci. Technol.*, 2013, **47**, 5074–5082.
7 A. Raza, B. Ding, G. Zainab, M. El-Newehy, S. S. Al-Deyab and J. Y. Yu, *J. Mater. Chem. A*, 2014, **2**, 10137–10145.
8 C. Luo and X. Heng, *Langmuir*, 2014, **30**, 10002–10010.
9 N. Ali, B. L. Zhang, H. B. Zhang, W. Zaman, X. J. Li, W. Li and Q. Y. Zhang, *Colloids Surf., A*, 2015, **472**, 38–49.
10 W. B. Zhang, Z. Shi, F. Zhang, X. Liu, J. Jin and L. Liang, *Adv. Mater.*, 2013, **25**, 2071–2076.
11 D. Deng, D. P. Prendergast, J. Macfarlane, R. Bagatin, F. Stellacci and P. M. Gschwend, *ACS Appl. Mater. Interfaces*, 2013, **5**, 774–781.
12 L. B. Zhang, Z. H. Zhang and P. Wang, *NPG Asia Mater.*, 2012, **4**, 1–8.
13 L. B. Zhang, Y. J. Zhong, D. Cha and P. Wang, *Sci. Rep.*, 2013, **4**, 2326–2340.
14 K. He, H. R. Duan, G. Y. Chen, X. K. Liu, W. S. Yang and D. Y. Wang, *ACS Nano*, 2015, **9**, 9188–9198.
15 Q. Wen, J. C. Di, L. Jiang, J. H. Yu and R. R. Xu, *Chem. Sci.*, 2013, **4**, 591–595.
16 B. Wang and Z. G. Guo, *Chem. Commun.*, 2013, **49**, 9416–9418.
17 N. Liu, Y. Z. Cao, X. Lin, Y. N. Chen, L. Feng and Y. Wei, *ACS Appl. Mater. Interfaces*, 2014, **6**, 12821–12826.
18 L. Wu, J. P. Zhang, B. C. Li and A. Q. Wang, *Polym. Chem.*, 2014, **5**, 2382–2390.
19 M. W. Lee, S. An, S. S. Latthe, C. M. Lee, S. Hong and S. S. Yoon, *ACS Appl. Mater. Interfaces*, 2013, **5**, 10597–10604.
20 J. P. Zhang and S. Seeger, *Adv. Funct. Mater.*, 2011, **21**, 4699–4704.
21 J. Wu, N. Wang, L. Wang, H. Dong, Y. Zhao and L. Jiang, *ACS Appl. Mater. Interfaces*, 2012, **4**, 3207–3212.
22 J. T. Wang, Y. Zheng and A. Q. Wang, *Chem. Eng. J.*, 2012, **213**, 1–7.
23 Z. J. Chen, K. Adil, Ł. J. Weseliński, Y. Belmabkhout and M. Eddaoudi, *J. Mater. Chem. A*, 2015, **3**, 6276–6281.
24 D. X. Xue, Y. Belmabkhout, O. Shekhah, H. Jiang, K. Adil, A. J. Cairns and M. Eddaoudi, *J. Am. Chem. Soc.*, 2015, **137**, 5034–5040.
25 H. Xu, Y. B. He, Z. J. Zhang, S. C. Xiang, J. F. Cai, Y. J. Cui and Y. Yang, *J. Mater. Chem. A*, 2013, **1**, 77–81.
26 S. H. Yang, A. G. Ramirez-Cuesta, R. Newby, V. Garcia-Sakai, P. Manuel, S. K. Callear and M. Schröder, *Nat. Chem.*, 2015, **7**, 121–129.
27 Z. R. Jiang, J. Ge, Y. X. Zhou, Z. Y. Wang, D. X. Chen, S. H. Yu and H. L. JIang, *NPG Asia Mater.*, 2016, **8**, 1–8.
28 R. Luebke, Y. Belmabkhout, Ł. J. Weseliński, A. J. Cairns, M. Alkordi, G. Norton, Ł. Wojtas, K. Adil and M. Eddaoudi, *Chem. Sci.*, 2015, **6**, 4095–4102.
29 A. H. Assen, Y. Belmabkhout, K. Adil, P. M. Bhatt, D. X. Xue, H. Jiang and M. Eddaoudi, *Angew. Chem., Int. Ed.*, 2015, **54**, 14353–14358.
30 J. F. Cai, J. C. Yu, H. L. Wang, X. Duan, Q. Zhang, C. D. Wu and G. D. Qian, *Cryst. Growth Des.*, 2015, **15**, 4071–4074.
31 H. M. Wen, B. Li, H. L. Wang, C. D. Wu, K. Alfooty, R. Krishna and B. L. Chen, *Chem. Commun.*, 2015, **51**, 5610–5613.
32 Z. J. Zhang, S. C. Xiang, X. T. Rao, Q. Zheng, F. R. Fronczek, G. D. Qian and B. L. Chen, *Chem. Commun.*, 2010, **46**, 7205–7207.
33 Z. R. Herm, B. M. Wiers, J. A. Mason, J. M. van Baten, M. R. Hudson, P. Zajdel, C. M. Brown, N. Masciocchi, R. Krishna and J. R. Long, *Science*, 2013, **340**, 960–964.
34 A. Cadiau, K. Adil, P. M. Bhatt, Y. Belmabkhout and M. Eddaoudi, *Science*, 2016, **353**, 137–140.
35 X. Duan, C. D. Wu, S. C. Xiang, W. Zhou, T. Yildirim, Y. J. Cui and G. D. Qian, *Inorg. Chem.*, 2015, **54**, 4377–4381.
36 B. L. Chen, S. C. Xiang and G. D. Qian, *Acc. Chem. Res.*, 2010, **43**, 1115–1124.
37 Y. X. Hu, S. C. Xiang, W. W. Zhang, Z. X. Zhang, L. Wang, J. F. Bai and B. L. Chen, *Chem. Commun.*, 2009, **45**, 7551–7553.
38 S. M. Chen, J. Zhang, T. Wu, P. Y. Feng and X. H. Bu, *J. Am. Chem. Soc.*, 2009, **131**, 16027–16029.
39 R. Ameloot, F. Vermoortele, W. Vanhove, M. B. J. Roeffaers, B. Sels and D. E. D. Vos, *Nat. Chem.*, 2011, **3**, 382–387.
40 L. J. Murray, M. Dincă and J. R. Jiang, *Chem. Soc. Rev.*, 2009, **36**, 1294–1314.
41 K. Sumida, D. L. Rogow, J. A. Mason, T. M. McDonald, E. D. Bloch, Z. R. Herm, T. H. Bea and J. R. Long, *Chem. Rev.*, 2012, **112**, 724–781.
42 B. Li, H. M. Wen, H. L. Wang, H. Wu, M. Tyagi, T. Yildirim, W. Zhou and B. L. Chen, *J. Am. Chem. Soc.*, 2014, **136**, 6207–6210.
43 B. L. Chen, N. W. Ockwig, A. R. Millward, D. S. Contreras and O. M. Yaghi, *Angew. Chem., Int. Ed.*, 2005, **117**, 4823–4827.

44 Y. B. He, R. Krishna and B. L. Chen, *Energy Environ. Sci.*, 2012, **5**, 9107–9120.
45 K. Srinivasu and S. K. Ghosh, *J. Phys. Chem.*, 2011, **115**, 16984–16991.
46 J. W. Brown, B. L. Henderson, M. D. Kiesz, A. C. Whallev, W. Morris, S. Grunder, H. X. Deng, H. Furukawa, J. I. Zink, J. F. Stoddart and O. M. Yaghi, *Chem. Sci.*, 2013, **4**, 2858–2864.
47 S. Saona, G. Savitha and J. N. Moorthy, *Inorg. Chem.*, 2015, **54**, 6829–6835.
48 B. Liu, D. S. Li, L. Hou, G. P. Yang, Y. Y. Wang and Q. Z. Shi, *Dalton Trans.*, 2013, **42**, 9822–9825.
49 S. T. Zheng, J. T. Bu, Y. F. Li, T. Wu, F. Zuo, P. Y. Feng and X. H. Bu, *J. Am. Chem. Soc.*, 2010, **132**, 17062–17064.
50 P. Z. Li, X. J. Wang, S. Y. Tan, C. Y. Ang, H. Chen, J. Liu, R. Zou and Y. Zhao, *Angew. Chem., Int. Ed.*, 2015, **54**, 12748–12752.
51 J. G. Nguyen and S. M. Cohen, *J. Am. Chem. Soc.*, 2010, **132**, 4560–4561.
52 K. Jayaramulu, K. K. R. Datta, C. Rçsler, M. Petr, M. Otyepka, R. Zboril and R. A. Fischer, *Angew. Chem., Int. Ed.*, 2016, **55**, 1178–1182.
53 C. Yang, U. Kaipa, Q. Z. Mather, X. P. Wang, V. Nesterov, A. F. Venero and M. A. Omary, *J. Am. Chem. Soc.*, 2011, **133**, 18094–18097.
54 T. H. Chen, I. Popov, O. Zanasni, O. Daugulis and O. Miljanic, *Chem. Commun.*, 2013, **49**, 4846–4848.
55 K. P. Rao, M. Higuchi, K. Sumida, S. Furukawa, J. G. Duan and S. Kitagawa, *Angew. Chem., Int. Ed.*, 2014, **53**, 8225–8230.
56 M. H. Zhang, L. L. Zhang, Z. Y. Xiao, Q. H. Zhang, R. M. Wang, F. N. Dai and D. F. Sun, *Sci. Rep.*, 2016, **6**, 1–10.
57 S. C. Xiang, W. Zhou, Z. J. Zhang, M. A. Green, Y. Liu and B. L. Chen, *Angew. Chem., Int. Ed.*, 2010, **49**, 4615–4618.
58 H. M. Wen, H. L. Wang, R. Krishna and B. L. Chen, *Chem. Commun.*, 2016, **52**, 1166–1169.
59 J. P. Zhang and X. M. Chen, *J. Am. Chem. Soc.*, 2009, **131**, 5516–5521.
60 Y. Yan, M. Jurícek, F. X. Coudert, N. A. Vermeulen, S. Grunder, A. Dailly and M. Schröder, *J. Am. Chem. Soc.*, 2016, **138**, 3371–3381.
61 M. C. Das, H. Xu, S. C. Xiang, Z. J. Zhang, H. D. Arman, G. D. Qian and B. L. Chen, *Chem.–Eur. J.*, 2011, **17**, 7817–7822.
62 Z. J. Zhang, S. C. Xiang, X. T. Rao, Q. Zheng, F. R. Fronczek, G. D. Qian and B. L. Chen, *Chem. Commun.*, 2010, **46**, 7205–7207.
63 Z. J. Zhang, S. C. Xiang and B. L. Chen, *CrystEngComm*, 2011, **13**, 5983–5992.
64 H. Xu, J. F. Cai, S. C. Xiang, Z. J. Zhang, C. D. Wu, X. T. Rao and G. D. Qian, *J. Mater. Chem. A*, 2013, **1**, 9916–9921.
65 W. Zhang, Y. L. Hu, J. Ge, H. L. Jiang and S. H. Yu, *J. Am. Chem. Soc.*, 2014, **136**, 16978–16981.
66 Z. J. Zhang, H. T. H. Nguyen, S. A. Miller, A. M. Ploskonka, J. B. Decoste and S. M. Cohen, *J. Am. Chem. Soc.*, 2016, **138**, 920–925.